SNAREpin/Munc18 promotes adhesion and fusion of large vesicles to giant membranes

David Tareste, Jingshi Shen, Thomas Melia, James Rothman

SNAREpin/Munc18 promotes adhesion and fusion of large vesicles to giant membranes

David Tareste, Jingshi Shen, Thomas J. Melia, and James E. Rothman*

Department of Physiology and Cellular Biophysics, Columbia University, 1150 St. Nicholas Avenue, New York, NY 10032

Contributed by James E. Rothman, December 26, 2007 (sent for review December 16, 2007)

Exocytic vesicle fusion requires both the SNARE family of fusion proteins and a closely associated regulatory subunit of the Sec1/Munc18 (SM) family. In principle, SM proteins could act at an early SNARE assembly step to promote vesicle–plasma membrane adhesion or at a late step to overcome the energetic barrier for fusion. Here, we use the neuronal cognates of each of these protein families to recapitulate, and distinguish, membrane adhesion and fusion on a novel lipidic platform suitable for imaging by fluorescence microscopy. Vesicle SNARE (v-SNARE) proteins reconstituted into giant vesicles (≈10 μm) are fully mobile and functional. Through confocal microscopy, we observe that large vesicles (≈100 nm) carrying target membrane SNAREs (t-SNAREs) both adhere to and freely move on the surface of the v-SNARE giant vesicle. Under conditions where the intrinsic ability of SNAREs to drive fusion is minimized, Munc18 stimulates both SNARE-dependent stable adhesion and fusion. Furthermore, mutation of a critical Munc18-binding residue on the N terminus of the t-SNARE syntaxin uncouples Munc18-stimulated vesicle adhesion from membrane fusion. We expect that the study of SNARE-mediated fusion with giant membranes will find wide applicability in distinguishing adhesion- and fusion-directed SNARE regulatory factors.

giant liposomes | Sec1/Munc18

Many vital cellular processes, including neuronal communication and insulin secretion, are governed by highly regulated fusion events between cargo-containing vesicles and target membranes. The core principle of intracellular membrane fusion is now well established (1, 2). First, the vesicles dock at target membranes, captured by Rab proteins and tethering factors. Next, the vesicles come into molecular contact with the target membranes as cognate v- and t-SNARE proteins, which initially reside in apposing bilayers, assemble in a zipper-like fashion to form a highly stable, partially structured, membrane-bridging complex called a SNAREpin (3–8). During membrane merging, the SNAREpin converts to a fully assembled SNARE complex that will ultimately reside in the single combined membrane. In addition to the SNAREs, the Sec1/Munc18 (SM) proteins are essential in every vesicle trafficking and fusion event, although the precise molecular mechanisms by which they exert their function are still elusive (9–11).

The fusion of synaptic vesicles with the presynaptic plasma membrane requires the v-SNARE protein VAMP2, the t-SNARE complex Syn1A/SNAP25, and the SM protein Munc18-1. Until recently, it was thought that Munc18-1 could only interact with the closed monomeric—and therefore fusion-incompetent—form of syntaxin-1A (12–14). However, new findings have demonstrated that Munc18-1 can also bind to the heterotrimeric SNARE complex (15–17). In addition, Munc18-1, like its yeast homolog Sec1, can enhance the kinetics and extent of SNARE-mediated membrane fusion *in vitro* (17, 18). This stimulation relies on a highly selective interaction of Munc18-1 with its neuronal cognate SNAREpin and thus imparts an additional layer of specificity to SNARE-dependent membrane fusion (17).

A comprehensive understanding of the fusion event requires the capacity to reconstitute the SNAREs into a wide variety of membrane platforms with tunable biophysical properties. By creating bilayer environments whose lipid composition, fluidity, membrane tension, and/or curvature can be controlled, one can account for the diversity observed across various cellular fusing compartments. In this regard, the reconstitution of SNAREs into small unilamellar vesicles (SUVs) provides tremendous flexibility and has offered great insights into the molecular mechanisms of SNARE-induced membrane fusion (6, 8, 17, 19–25). However, SUVs display an intrinsically high degree of membrane curvature and tension, biophysical properties which strongly influence the energetics of fusion and which are essentially invariant in this system. Furthermore, because of their small size, SUVs are generally beyond the detection limit of optical approaches used to study either functional membrane domains or single fusion events. Recent biophysical advances now allow the reconstitution of large (≈100 nm) or giant (≈10 μm) unilamellar vesicles (LUVs or GUVs) bearing functional transmembrane proteins, whose distribution, mobility, and biological activity can be monitored by optical microscopy (26–30).

In this article, we reconstitute t-SNARE complexes into LUVs, reconstitute v-SNARE proteins into GUVs, and present an assay that allows us to follow adhesion and fusion of these t-LUVs to the v-GUVs in the absence or the presence of the fusion activator Munc18-1 (unless otherwise specified, t- and v-SNARE will denote the plasma membrane complex Syn1A/SNAP25 and the synaptic vesicle protein VAMP2, respectively). The approach developed here will be applicable to the study of many other regulatory factors known to modulate SNARE assembly and membrane fusion.

Results

Activity and Mobility of v-SNAREs in Giant Membranes. A comprehensive description of the lipid and protein composition of synaptic vesicles has recently been reported (31). Using this study as a guide, we prepared our v-GUVs by a modified electroformation method (26, 28), starting from small proteoliposomes of v-SNAREs at a theoretical lipid-to-protein ratio of 200 [supporting information (SI) Fig. 5*A*]. Unless otherwise noted, the experiments presented here used v-GUVs consisting of 60 mol % phosphatidylcholine (DOPC), 10 mol % phosphatidylserine (DOPS) and 30 mol % phosphatidylethanolamine (DOPE). Neither the vesicle adhesion nor the fusion events described below were significantly altered when liposomes were prepared without DOPE (SI Fig. 10*A*).

The activity of v-SNARE proteins when embedded into the membrane of GUVs was assessed through binding to a fluorescent and soluble version of their t-SNARE partner (EYFP-SNAP25/Syn1A-ΔTM protein). Most v-GUVs (>90%) were

Author contributions: D.T., J.S., T.J.M., and J.E.R. designed research; D.T. performed research; D.T. and J.S. contributed new reagents/analytic tools; D.T. and J.E.R. analyzed data; and D.T. and T.J.M. wrote the paper.

The authors declare no conflict of interest.

*To whom correspondence should be addressed. E-mail: jr2269@columbia.edu.

This article contains supporting information online at www.pnas.org/cgi/content/full/0712125105/DC1.

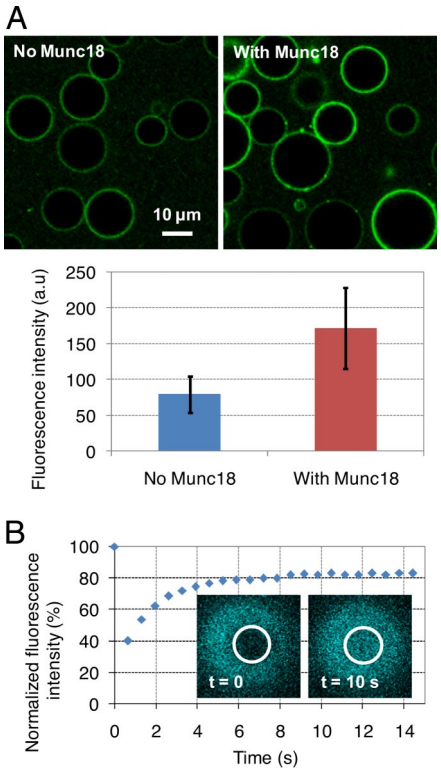

Fig. 1. Activity and mobility of v-SNAREs reconstituted into DOPC:DOPS-:DOPE (60:10:30) GUVs. (*A*) Binding of EYFP-SNAP25/Syn1A-ΔTM (0.1 μM) to v-GUVs in the absence or the presence of 2 μM Munc18-1, after 2 h of incubation at room temperature. Munc18-1 clearly promotes the formation of SNARE complexes; average values and standard deviations are from $n = 40–60$ GUVs. (*B*) FRAP experiments on DOPC:DOPS (90:10)/ECFP-VAMP2 GUVs (theoretical lipid-to-protein ratio = 200). Bleaching was performed at the top of the GUV. v-SNAREs are fully mobile in the GUV membrane with an average diffusion coefficient of 3.4 $\mu m^2/s$; after recovery, the fluorescence does not reach 100% because of (*i*) the overall loss of fluorescence in the GUV membrane after bleaching (≈5–10% depending on the disk and the GUV size) and (*ii*) the intrinsic photobleaching of the ECFP probe that occurs during reading (≈10%).

able to bind to this fluorescent cognate t-SNARE (Fig. 1*A Left*). To test whether Munc18-1 could promote SNARE complex formation in our system, v-GUVs were next incubated with EYFP-SNAP25/Syn1A-ΔTM in the presence of Munc18-1 in solution. The extent of EYFP-SNAP25/Syn1A-ΔTM binding was increased by ≈2-fold in the presence of Munc18-1 (Fig. 1*A Right*), indicating that Munc18-1 can readily stimulate the assembly of *cis*-SNARE complexes on GUV membranes. The surface density of these *cis*-SNARE complexes (and thus of active v-SNAREs) was estimated by Western blot analysis of Ni-NTA beads functionalized with His-tagged EYFP-SNAP25/Syn1A-ΔTM and displaying the same fluorescence intensity (SI Fig. 5*B*). By this approach, our v-GUVs include ≈5,500 active v-SNAREs per μm^2 (i.e., ≈1 protein for 320 lipids). This is consistent with the theoretical lipid-to-protein ratio used during liposome preparation and slightly lower than the physiological density of v-SNAREs in synaptic vesicles [≈12,600 v-SNAREs per μm^2 (31)].

To measure the lateral mobility of v-SNAREs within the GUV bilayers, we performed fluorescence recovery after photobleaching (FRAP) experiments on GUVs bearing a fluorescent version of the v-SNARE protein (ECFP-VAMP2). ECFP-VAMP2 proteins were fully mobile in the GUV membrane with a diffusion coefficient of 3.4 ± 0.6 $\mu m^2/s$ (Fig. 1*B*), which is very similar to that measured for a fluorescent lipid under the same experimental conditions (SI Fig. 6*A*).

Munc18-1 Promotes Adhesion and Fusion of t-LUVs to v-GUVs. We have previously demonstrated that neuronal SNAREs can drive the fusion of small liposomes (8) and that these fusion events can be strongly activated by Munc18-1 (17). Here, we wanted to investigate whether SNAREs and Munc18-1 could still promote fusion when much larger membranes were involved. We chose to fuse LUVs to GUVs, a system that offers the possibility to monitor both vesicle adhesion and fusion by optical microscopy (32, 33).

t-LUVs were prepared by detergent-assisted direct incorporation of t-SNAREs into preformed protein-free LUVs consisting of 55 mol % DOPC, 10 mol % DOPS, 30 mol % DOPE, and 5 mol % phosphatidylethanolamine (Lissamine Rhodamine B) (DOPE-RHO); their theoretical lipid-to-protein ratio was 400 (SI Fig. 5*A*), a density similar to that we previously used to demonstrate the activation of SNARE-mediated liposome fusion by Munc18-1 (17). Vesicle adhesion and fusion were both quantified after incubation and rinsing of unbound t-LUVs. The fusion of t-LUVs into v-GUVs was measured by a lipid-mixing assay, following the transfer of fluorescent lipids from the t-LUV membrane, which initially contained 5 mol % DOPE-RHO, to the v-GUV membrane, which was initially nonfluorescent. Adhesion of t-LUVs onto v-GUVs was estimated by counting the number of bright dots sitting and moving (SI Movie 1) on the dimmer fluorescent background of v-GUV membranes. To quantify t-LUV/v-GUV lipid mixing, one requires (*i*) a calibration curve for the fluorescence intensity of a GUV as a function of the mol % of DOPE-RHO lipids in its membrane and (*ii*) an accurate measure of the size of both t-LUVs and v-GUVs. The calibration curve was obtained by measuring the fluorescence intensity of protein-free GUVs containing various controlled amounts of DOPE-RHO in their bilayer (Fig. 2*B* and SI Fig. 7). The average size of t-LUVs was determined by cryo-electron microscopy [(88 ± 21) nm (Fig. 2*A*)], and the size of v-GUVs was directly measured from the confocal pictures of each sample tested.

v-GUVs were first incubated with t-LUVs in the absence of Munc18-1. After careful rinsing, the membranes of v-GUVs were decorated with only a few t-LUVs [2 ± 1 (Fig. 3*A Left* and Table 1); note that, because the number of bound t-LUVs was counted on equatorial sections of v-GUVs, it cannot be considered absolute and is likely an underestimate]. At a higher density of SNAREs, the number of bound t-LUVs increased significantly, and when v-GUVs were incubated with protein-free LUVs, stable vesicle adhesion did not occur (SI Fig. 8 and SI Table 2). When t-LUVs and v-GUVs were incubated together with Munc18-1, the number of bound t-LUVs was also significantly higher [6 ± 3 (Fig. 3*A Right* and Table 1)]. This stimulation of vesicle binding by Munc18-1 required both SNARE partners to be present on the membranes (SI Table 2). This result thus confirms and extends the above binding experiments (Fig. 1*A*): Munc18-1 not only promotes the formation of *cis*-SNARE complexes, it can also stimulate the formation of membrane-bridging SNAREpins across our large membranes.

In addition to binding events of t-LUVs onto v-GUVs, fusion events can also be measured in this system as indicated by the development of a continuous fluorescent background within the membrane of all v-GUVs (Fig. 3*A*). SNARE proteins could slightly promote large/giant membrane fusion at 37°C compared with a control experiment in which t-SNAREs were absent from the LUV bilayer (Fig. 3*C*). The occurrence of fusion was further validated by FRAP experiments showing that DOPE-RHO lipids transferred into the v-GUV membrane displayed unrestricted Brownian motion with an average diffusion coefficient of 2.3 $\mu m^2/s$ (SI Fig. 6*B*).

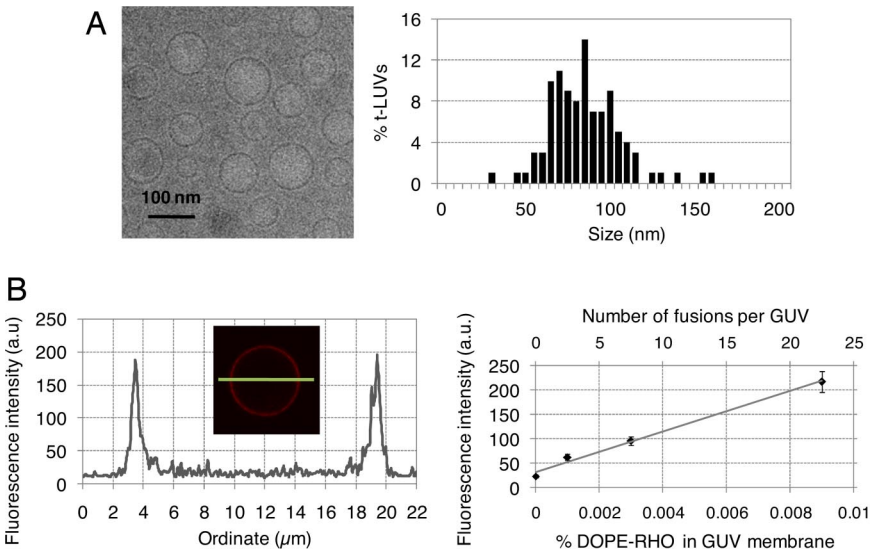

Fig. 2. Fusion calibration. (*A*) Representative cryo-electron microscopy picture and size distribution of DOPC:DOPS:DOPE:DOPE-RHO (55:10:30:5)/t-SNAREs LUVs (n = 109 liposomes); the average size is 88 nm. (*B Left*) Fluorescence intensity across the equatorial section of a protein-free GUV containing 0.009 mol % DOPE-RHO (typical profile used for calibrating and estimating the number of fusion events). (*B Right*) Fluorescence intensity of protein-free GUVs as a function of the mol % DOPE-RHO in their membrane (lower x axis), and conversion to the number of LUVs fusing per GUV (upper x axis), in the case of 90-nm LUVs and 10-μm v-GUVs. The titration was conducted for 0 < mol % DOPE-RHO < 0.24, using lower confocal gain settings when the fluorescence intensity (scaled from 0 to 255) reached saturation (SI Fig. 7). To analyze LUV/GUV fusion, the upper x axis of these calibration curves (number of fusion events) was corrected to account for the actual size of each GUV tested.

Both the kinetics and the total number of fusion events could be strongly enhanced (by ≈4-fold) in the presence of Munc18-1 (Fig. 3 *B* and *C*). When experiments were conducted at room temperature, the fusion induced by SNAREs was indistinguishable from SNAREpin-independent fusion reactions (fusion reactions where either or both membranes were devoid of SNAREs). Even under this more stringent temperature condition, Munc18-1 was still able to promote SNARE-dependent fusion of our large/giant membranes, but only when SNAREs were present in both interacting membranes (SI Fig. 9*A*).

Protein Determinants of Munc18-1 Function. Next, we examined whether Munc18-1 could still simulate fusion of our large/giant membranes when other, nonneuronal, SNAREs were involved. To test this, we reconstituted the late endosomal v-SNARE protein VAMP8 into GUVs and challenged these VAMP8-

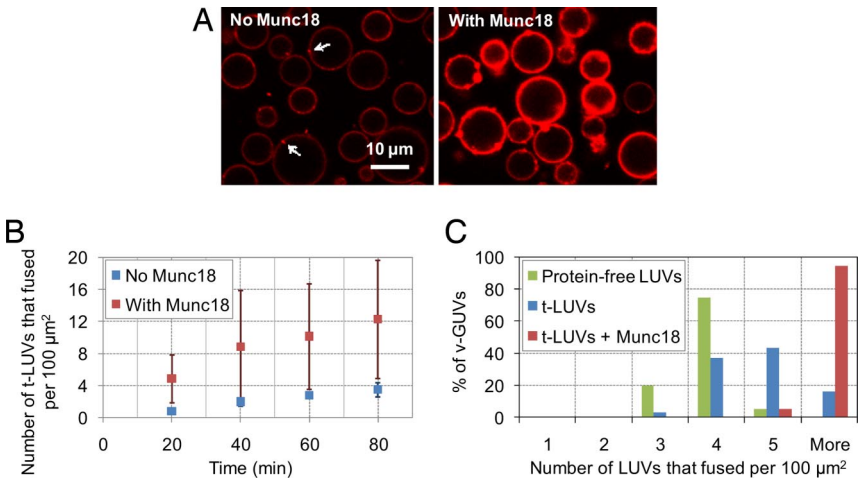

Fig. 3. Munc18-1 activates t-LUV/v-GUV adhesion and fusion. (*A*) Confocal imaging of DOPC:DOPS:DOPE (70:10:20)/v-SNARE GUVs after 2 h of incubation at 37°C with 5 μM DOPC:DOPS:DOPE:DOPE-RHO (65:10:20:5)/t-SNARE LUVs in the absence or the presence of 2 μM Munc18-1 [both pictures were taken with the same settings as in Fig. 2; fusion in the presence of Munc18-1 was quantified from pictures at lower confocal gain settings (see SI Fig. 7)]. Some bound liposomes are indicated by the arrows. To estimate the number of fusion events, three lines similar to that displayed in Fig. 2*A* were drawn across the equator of v-GUVs, avoiding bound liposomes. (*B*) Fusion kinetics at 37°C in the absence or the presence of 2 μM Munc18-1 (each data point gives the average value over n = 7–12 GUVs observed within 5 min). In the presence of Munc18-1, the fusion kinetics are enhanced ≈4-fold. (*C*) Distribution of fusion events at 37°C across the population of v-GUVs after 2 h of incubation at 37°C with protein-free LUVs (green) or t-LUVs in the absence (blue) or presence (red) of Munc18-1 (histograms from n = 40–60 GUVs). The average number of fusion events per 100 μm^2 of v-GUV membrane is 3 ± 1 with protein-free LUVs, 4 ± 1 with t-LUVs in the absence of Munc18-1, and 14 ± 6 with t-LUVs in the presence of Munc18-1 (see also SI Fig. 10*B*, which gives the complete distribution of fusion events). Munc18-1 thus increases SNAREpin-dependent fusion efficiency by ≈10-fold (after subtraction of basal fusion).

Table 1. Munc18-dependent stimulation of t-LUVs adhesion to v-GUVs (see legend of Fig. 4 for experimental details)

	T + V2	T + V8	ΔN-T + V2	L8A-T + V2
No Munc18	2 ± 1	4 ± 1	2 ± 1	2 ± 1
With Munc18	6 ± 3	1 ± 1	2 ± 2	6 ± 3

The number of bound t-LUVs was counted on equatorial sections of v-GUVs.

GUVs with EYFP-SNAP25/Syn1A-ΔTM proteins or t-LUVs. VAMP8-GUVs were able to bind EYFP-SNAP25/Syn1A-ΔTM and to capture t-LUVs with the same—and even slightly higher—efficiency as v-GUVs (Table 1 and SI Fig. 9*B*). Fusion of t-LUVs with VAMP8-GUVs was, however, slightly lower than that observed with v-GUVs. In addition, neither adhesion nor fusion of t-LUVs to VAMP8-GUVs could be further activated by Munc18-1 (Fig. 4*A* and Table 1). The adhesion of t-LUVs to VAMP8-GUVs was almost inexistent in the presence of Munc18-1, suggesting that the complex Munc18-1/t-SNARE exclusively binds to its cognate v-SNARE.

The N-terminal domain of Syn1A, and more specifically the leucine residue at position 8, is absolutely required for Munc18-1 activation of SNARE-mediated liposome fusion (17). In our t-LUV/v-GUV system, when the whole N-terminal domain of Syn1A was removed (ΔN-t-SNARE mutant), Munc18-1 was unable to promote either vesicle adhesion or membrane fusion. Interestingly, when the leucine residue was mutated into an alanine (L8A-t-SNARE mutant), Munc18-1 could still activate t-LUVs adhesion onto v-GUVs but could not stimulate membrane fusion (Fig. 4*B* and Table 1). This result suggests that Munc18-1 may stimulate both SNAREpin formation and SNARE-mediated fusion and that, in this optical system, its role in vesicle adhesion can be uncoupled (and easily distinguished) from its role in fusion activation.

Discussion

There are many properties beyond simply protein and lipid composition that determine the fusogenic potential of individual membranes. In particular, membrane tension and/or curvature, and the formation of distinct localized architectures (including protein clusters, membrane dimples, and lipid rafts) all appear to influence the rate and extent of membrane fusion. For example, high bilayer curvature significantly increases fusion efficiency in various protein-free liposome fusion reactions, driven by divalent cations or poly(ethylene glycol) (PEG) (34, 35). There is no single reconstitution method that puts each of these variables in play, and as such, there continues to be a need for new and multiple assay systems. To bridge this reconstitution gap, we have explored the potential of large/giant liposome membranes. In our LUV/GUV system, SNAREs could only moderately promote membrane fusion, compared with SNAREpin-independent fusion reactions. We suspect that this is due to a high energetic barrier for fusion resulting from (*i*) the size of the fusing objects, which display low membrane curvature and thus expose less hydrophobic regions than—for instance, highly curved small liposomes—and (*ii*) the low surface density of SNAREs used here. The effect of size has some precedent in the study of viral fusogens—where, for example, the hemagglutinin fusion peptide (HA) was able to induce fusion of LUVs but showed no fusogenic activity on GUVs (36). Membrane fusion is highly dependent on SNARE surface density such that liposome fusion efficiency increases as the protein-to-lipid ratio increases (unpublished work). Although we aimed to work near physiological v-SNARE densities as determined for synaptic vesicle membrane (31), the actual concentration of v-SNAREs after reconstitution turned out to be slightly lower than expected (1 protein for 320 lipids). The physiological surface density of t-SNAREs is not known, but these proteins are found in clusters in cells (37, 38), suggesting a very high local concentration at the site of fusion (likely higher than the 1 protein for 520 lipids used here). Overall, we would suggest that our LUV/GUV system represents a more stringent test of SNARE-dependent fusion with the possibility to clearly reveal the effect of any potential fusion activator. Importantly, reconstitution into GUVs allows full mobility of the incorporated SNAREs, with diffusion coefficients comparable to those expected for single proteins, and thus, in this system, rampant protein aggregation is not occurring. An exciting avenue for further research made possible by the sheer size of our GUVs will be to direct the clustering of

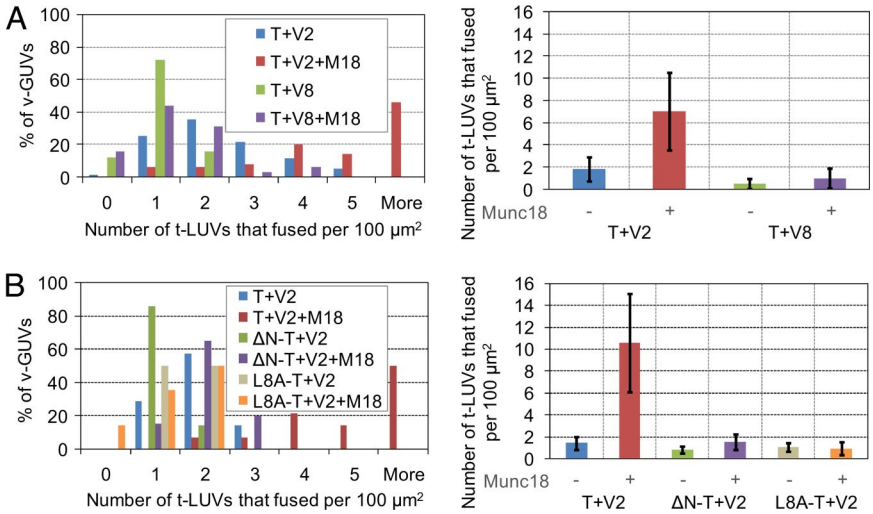

Fig. 4. Munc18-1 specifically activates neuronal SNARE pairs and requires the N-terminal peptide of Syn1A. (*A*) DOPC:DOPS:DOPE:DOPE-RHO (55:10:30:5)/t-SNARE LUVs (5 μM) were added to DOPC:DOPS:DOPE (60:10:30)/v-SNARE or VAMP8 GUVs, and the reaction was incubated for 2 h at room temperature in the absence or presence of 2 μM Munc18-1 (histograms from $n = 80–100$ GUVs). Neither vesicle adhesion (Table 1) nor fusion of t-LUVs to VAMP8-GUVs is promoted by Munc18-1. (*B*) DOPC:DOPS:DOPE (60:10:30)/v-SNARE GUVs were incubated for 2 h at room temperature with 5 μM DOPC:DOPS:DOPE:DOPE-RHO (55:10:30:5) LUVs of t-SNAREs, ΔN-t-SNAREs, or L8A-t-SNAREs in the absence or the presence of 2 μM Munc18-1 (histograms from $n = 20–40$ GUVs). Neither vesicle adhesion (Table 1) nor fusion is activated in the case of the N-terminally deleted t-SNARE mutant. In the case of the L8A-Syn1A mutant, Munc18-1 does not activate fusion but still promotes vesicle adhesion (Table 1).

these mobile SNARE proteins—for example, by altering lipid composition (26, 39)—into local sites of high protein surface density, which will better mimic the *in vivo* circumstance and perhaps yield highly efficient localized membrane fusion.

SM proteins have long been known to play a central role in membrane traffic and to coordinate closely with SNARE proteins, particularly syntaxins (9–11). Our reconstitution studies now suggest that rather than a peripherally important regulatory protein, Munc18-1 is perhaps better considered an essential member of the SNAREpin membrane fusion machinery. Results obtained with this new LUV/GUV system are concordant with our recent study involving SUVs (17); both studies demonstrate that Munc18-1 exerts its activating effect by selectively interacting with its neuronal cognate SNAREpin, and through interactions involving the N-terminal sequence of Syn1A. The conditions used here can be considered highly stringent, such that basal SNARE-mediated fusion is almost inexistent. In this circumstance, Munc18-1 plays an essential role in driving membrane fusion. These reconstitution approaches mesh well with numerous lines of evidence obtained from *in vivo* studies, where null mutations of either the SNARE or the Munc18-1 gene result in a severe reduction of synaptic vesicle exocytosis (10, 40–42), placing both families at the same late step of the fusion process.

How Munc18-1 functions remains to be established, but some clues may be gleaned from its unique structure. The U-shape geometry of Munc18-1 is conformationally appropriate to act as a stabilizer of the SNARE four-helix bundle during SNAREpin assembly and indeed has already been shown to accommodate a bundle assembly when bound to the closed form of Syn1A (14). Although the leucine residue at position 8 of Syn1A is essential for binding to *cis*-SNAREs in solution and for activation of liposome-mediated fusion, it is dispensable for binding to *cis*-SNAREs on liposomes (17). Here, we show that this residue is also not essential for the Munc18-1-stimulated accumulation of bound vesicles in the LUV/GUV system, suggesting that other regions (presumably the coiled-coil domains) of the SNAREpin present a suitable binding site for Munc18-1, and that stimulation of vesicle adhesion can be functionally uncoupled from stimulation of fusion. Thus, Munc18-1 may act by increasing the binding energy of cognate SNAREs in two stages: first, to reduce the number of nonproductive collisions that inevitably occur when a vesicle encounters its target membrane; and second, to drive productive SNARE complexes to completion. Overall, the Munc18-1/SNAREpin complex might constitute a membrane bridging complex of higher stabilization energy that is able to overcome the high energetic barrier for fusion imposed by large membranes.

GUVs offer the possibility of following vesicle adhesion and fusion independently in the same experiment without the complications that can arise from substrate supports (like aberrant interactions of transmembrane proteins with the underlying glass). As we begin to elucidate functions of other critical players, such as synaptotagmins and complexins (43), it becomes increasingly important to determine both the temporal and spatial elements of the mechanism of regulation and to distinguish between vesicle docking, priming, and fusion as intermediates. Establishing SNARE-mediated fusion to a GUV is a first step toward developing a system where the manipulation of membrane tension, curvature, and localized architecture needed to mimic the complexity of regulated exocytic sites might be possible.

Methods

Chemicals, protein purifications, and cryo-electron microscopy are presented in *SI Methods*.

Reconstitution of t-SNAREs into LUVs. t-LUVs were prepared by direct incorporation of t-SNARE complexes into preformed protein-free large liposomes (30). These large liposomes were prepared by the extrusion method; 7.5 μmol of a lipid mixture (in chloroform) consisting of 55 mol % DOPC, 10 mol % DOPS, 30 mol % DOPE, and 5 mol % DOPE-RHO was dried in a glass tube for 15 min under a gentle stream of nitrogen, and for 1 h under vacuum. The dried lipid film was resuspended in 500 μl of 25 mM Hepes/KOH (pH 7.5)/100 mM KCl/10% (vol/vol) glycerol by vigorously vortexing for 1 h at room temperature. The multilamellar liposomes were frozen in liquid nitrogen for 30 s and then thawed in a 37°C water bath for 3 min. This cycle was repeated seven times. LUVs were produced by extrusion through two 400-nm polycarbonate membranes, using a LiposoFast extruder from Avestin (at least 19 passages); 100 μl of these LUVs were incubated with 200 μl of t-SNAREs diluted in buffer A [25 mM Hepes/KOH (pH 7.5), 100 mM KCl, 10% (vol/vol) glycerol, 1% β-OG, 1 mM DTT], under gentle vortexing for 1 h at room temperature. The mixture was diluted two times in buffer B [25 mM Hepes/KOH (pH 7.5), 100 mM KCl, 10% (vol/vol) glycerol, 1 mM DTT]. Detergent was removed by flow-dialysis against buffer B (≈3.3 ml/min for ≈20 h at 4°C). These t-LUVs could be kept on ice for up to 2 weeks without losing activity.

Reconstitution of v-SNAREs into GUVs. v-GUVs were prepared by a modified electroformation method (26, 28), starting from small liposomes of v-SNAREs made by the standard method (8); 1.5 μmol of a lipid mixture (in chloroform) consisting of 60 mol % DOPC, 10 mol % DOPS, and 30 mol % DOPE was dried in a glass tube for 15 min under a gentle stream of nitrogen, and for 1 h under vacuum. The dried lipid film was resuspended in 200 μl of v-SNAREs diluted in buffer A, under vigorous vortexing for 1 h at room temperature. The mixture was diluted three times in buffer B. Detergent was removed by flow-dialysis against buffer B (≈3.3 ml/min for ≈20 h at 4°C). These v-SUVs were kept at −80°C. To generate v-GUVs, a 50-μl aliquot of v-SUVs was thawed, mixed with 950 μl of rinsing buffer [25 mM Hepes/KOH (pH 7.5), 100 mM KCl, 1 mM DTT], and spun at 200,000 × *g* for 2 h at 4°C; 950 μl of supernatant was removed, and the pellet was left on ice for 20 min. Liposomes were resuspended in 50 μl of rinsing buffer, deposited on indium tin oxide (ITO) conductive plaques (30 Ω) by drops of 1 μl, and dried under vacuum for 1 h. Dried lipid films were rehydrated at 37°C with sucrose at 220 mOsm in 10% (vol/vol) glycerol, applying the following sinusoidal electric fields: 8 Hz, 50, 100, 200, 300, 500, 700, and 900 mV for 6 min each; 8 Hz, 1.1 V for 2 h; and 4 Hz, 1.5 V for 30 min. v-GUVs were allowed to cool down at room temperature for 30 min and kept overnight at 4°C before being harvested. These v-GUVs could be kept on ice for up to 2 weeks without losing activity. Reconstitution of t-SNAREs into GUVs, using the same protocol [including variations involving partial-dehydration (28) or dehydration in the presence of sucrose (27)] led to highly variable levels of active t-GUVs, with sometimes only 10% of all t-GUVs that could bind to their cognate v-SNAREs. Because such variability largely complicated statistical analysis of fusion events, we focused on v-GUVs.

Binding, Adhesion, Fusion, and FRAP Assays. All images were acquired on the confocal microscope TCS SP2 from Leica, equipped with LCS software and using a HCX PL APO ×63/1.40–0.60 oil objective [zoom, ×4; beam expander, 3; pinhole, 200 μm; scan speed, 400 Hz, except during FRAP experiments (1,000 Hz)]. Samples were prepared in glass-bottom dishes (P35G-1.5-14-C; MatTek) coated with 10% (wt/vol) BSA for 1 h at room temperature. For binding experiments (λ_{exc} = 514 nm; λ_{em} = 522–603 nm), 100 μl of v-GUVs was added to a 200-μl solution of 0.1 μM EYFP-SNAP25/Syn1A-ΔTM +/− 2 μM Munc18-1 in buffer B and incubated at room temperature for the indicated time periods; observations were conducted without rinsing. For adhesion/fusion experiments (λ_{exc} = 543 nm; λ_{em} = 551–633 nm), 100 μl of v-GUVs was added to a 200-μl solution of 5 μM t-LUVs +/− 2 μM Munc18-1 in buffer B and incubated at room temperature or at 37°C for the indicated time periods. Samples were rinsed before observation: (*i*) the central 300-μl drop was slowly grown to 1 ml by addition of buffer B to its edges; (*ii*) 3 ml of buffer B was gently added from the side of the dish, and the solution was mixed by slow up-and-down pipetting (≈4 ml/min); 3 ml was then slowly removed from the dish, and the rinsing step (*ii*) was repeated three times. Fusion was quantified by using the titration curves $I_{fluo} = f$ (mol % DOPE-RHO) obtained with three distinct confocal gain settings (PMT voltage = 550, 450, or 350) to cover the range 0 < mol % DOPE-RHO < 0.24 (Fig. 2*B* and SI Fig. 7). Larger standard deviations were usually obtained in the presence of Munc18-1, reflecting some heterogeneity of behavior within the population of v-GUVs. The origin of this heterogeneity is not clear but might be accounted for by subpopulations of v-GUVs with lower affinity for Munc18-1. FRAP experiments (λ_{exc} = 458 nm; λ_{em} = 465–600 nm for ECFP; as above for DOPE-RHO) were conducted either at the top or at the bottom of GUVs by photobleaching a fluorescent disk in the lipid membrane (one scan at maximum laser power); recovery was monitored at 5–10% of the maximum laser power (one picture every 657 ms). Recovery curves (average over at least five consecutive FRAP experiments on the same region) were fit with the software Mathematica, using modified Bessel functions (44, 45), which gives the characteristic diffusion time τ. Diffusion coefficients, *D*, were deduced by testing at least 2 disk radius, usually r = 3.5 μm and 7 μm, and using the relation: $D = r^2/4\tau$.

ACKNOWLEDGMENTS. We thank B. Rice, J. Berriman, and K. Derr of the New York Structural Biology Center, who facilitated our work on the cryo-electron microscope. We also thank Avram Slovic, Frédéric Pincet, and Hong Ji for experimental help and many fruitful discussions. This work was supported by the Human Frontier Science Program, a travel grant from the National Science Foundation, and National Institutes of Health grants to James E. Rothman.

1. Pfeffer SR (2007) Unsolved mysteries in membrane traffic. *Annu Rev Biochem* 76:629–645.
2. Waters MG, Hughson FM (2000) Membrane tethering and fusion in the secretory and endocytic pathways. *Traffic* 1:588–597.
3. Hanson PI, Roth R, Morisaki H, Jahn R, Heuser JE (1997) Structure and conformational changes in NSF, its membrane receptor complexes visualized by quick-freeze/deep-etch electron microscopy. *Cell* 90:523–535.
4. Hu C, *et al.* (2003) Fusion of cells by flipped SNAREs. *Science* 300:1745–1749.
5. Li F, *et al.* (2007) Energetics and dynamics of SNAREpin folding across lipid bilayers. *Nat Struct Mol Biol* 14:890–896.
6. Melia TJ, *et al.* (2002) Regulation of membrane fusion by the membrane-proximal coil of the t-SNARE during zippering of SNAREpins. *J Cell Biol* 158:929–940.
7. Sollner T, Bennett MK, Whiteheart SW, Scheller RH, Rothman JE (1993) A protein assembly-disassembly pathway in-vitro that may correspond to sequential steps of synaptic vesicle docking, activation, and fusion. *Cell* 75:409–418.
8. Weber T, *et al.* (1998) SNAREpins: Minimal machinery for membrane fusion. *Cell* 92:759–772.
9. Burgoyne RD, Morgan A (2007) Membrane trafficking: Three steps to fusion. *Curr Biol* 17:R255–R258.
10. Rizo J, Sudhof TC (2002) SNAREs and Munc18 in synaptic vesicle fusion. *Nat Rev Neurosci* 3:641–653.
11. Toonen RF, Verhage M (2007) Munc18-1 in secretion: Lonely Munc joins SNARE team and takes control. *Trends Neurosci* 30:564–572.
12. Dulubova I, *et al.* (1999) A conformational switch in syntaxin during exocytosis: Role of munc18. *EMBO J* 18:4372–4382.
13. Hata Y, Slaughter CA, Sudhof TC (1993) Synaptic vesicle fusion complex contains unc-18 homolog bound to syntaxin. *Nature* 366:347–351.
14. Misura KM, Scheller RH, Weis WI (2000) Three-dimensional structure of the neuronal-Sec1-syntaxin 1a complex. *Nature* 404:355–362.
15. Dulubova I, *et al.* (2007) Munc18-1 binds directly to the neuronal SNARE complex. *Proc Natl Acad Sci USA* 104:2697–2702.
16. Rickman C, Medine CN, Bergmann A, Duncan RR (2007) Functionally and spatially distinct modes of munc18-syntaxin 1 interaction. *J Biol Chem* 282:12097–12103.
17. Shen JS, Tareste DC, Paumet F, Rothman JE, Melia TJ (2007) Selective activation of cognate SNAREpins by Sec1/Munc18 proteins. *Cell* 128:183–195.
18. Scott BL, *et al.* (2004) Sec1p directly stimulates SNARE-mediated membrane fusion in vitro. *J Cell Biol* 167:75–85.
19. McNew JA, *et al.* (2000) Close is not enough: SNARE-dependent membrane fusion requires an active mechanism that transduces force to membrane anchors. *J Cell Biol* 150:105–117.
20. Hu K, *et al.* (2002) Vesicular restriction of synaptobrevin suggests a role for calcium in membrane fusion. *Nature* 415:646–650.
21. Schuette CG, *et al.* (2004) Determinants of liposome fusion mediated by synaptic SNARE proteins. *Proc Natl Acad Sci USA* 101:2858–2863.
22. Tucker WC, Weber T, Chapman ER (2004) Reconstitution of Ca^{2+}-regulated membrane fusion by synaptotagmin and SNAREs. *Science* 304:435–438.
23. Lu X, Zhang F, McNew JA, Shin YK (2005) Membrane fusion induced by neuronal SNAREs transits through hemifusion. *J Biol Chem* 280:30538–30541.
24. Melia TJ, You DQ, Tareste DC, Rothman JE (2006) Lipidic antagonists to SNARE-mediated fusion. *J Biol Chem* 281:29597–29605.
25. Vicogne J, *et al.* (2006) Asymmetric phospholipid distribution drives in vitro reconstituted SNARE-dependent membrane fusion. *Proc Natl Acad Sci USA* 103:14761–14766.
26. Bacia K, Schuette CG, Kahya N, Jahn R, Schwille P (2004) SNAREs prefer liquid-disordered over ''raft'' (liquid-ordered) domains when reconstituted into giant unilamellar vesicles. *J Biol Chem* 279:37951–37955.
27. Doeven MK, *et al.* (2005) Distribution, lateral mobility and function of membrane proteins incorporated into giant unilamellar vesicles. *Biophys J* 88:1134–1142.
28. Girard P, *et al.* (2004) A new method for the reconstitution of membrane proteins into giant unilamellar vesicles. *Biophys J* 87:419–429.
29. Manneville JB, Bassereau P, Levy D, Prost J (1999) Activity of transmembrane proteins induces magnification of shape fluctuations of lipid membranes. *Phys Rev Lett* 82:4356–4359.
30. Rigaud JL, Levy D (2003) Reconstitution of membrane proteins into liposomes. *Methods Enzymol* 372:65–86.
31. Takamori S, *et al.* (2006) Molecular anatomy of a trafficking organelle. *Cell* 127:831–846.
32. Marchi-Artzner V, *et al.* (2001) Selective adhesion, lipid exchange and membrane-fusion processes between vesicles of various sizes bearing complementary molecular recognition groups. *ChemPhysChem* 2:367–376.
33. Kahya N, Pecheur EI, de Boeij WP, Wiersma DA, Hoekstra D (2001) Reconstitution of membrane proteins into giant unilamellar vesicles via peptide-induced fusion. *Biophys J* 81:1464–1474.
34. Nir S, Wilschut J, Bentz J (1982) The rate of fusion of phospholipid-vesicles and the role of bilayer curvature. *Biochim Biophys Acta* 688:275–278.
35. Lentz BR, Mcintyre GF, Parks DJ, Yates JC, Massenburg D (1992) Bilayer curvature and certain amphipaths promote poly(ethylene glycol)-induced fusion of dipalmitoylphosphatidylcholine unilamellar vesicles. *Biochemistry* 31:2643–2653.
36. Nomura F, *et al.* (2004) Microscopic observations reveal that fusogenic peptides induce liposome shrinkage prior to membrane fusion. *Proc Natl Acad Sci USA* 101:3420–3425.
37. Lang T, *et al.* (2001) SNAREs are concentrated in cholesterol-dependent clusters that define docking and fusion sites for exocytosis. *EMBO J* 20:2202–2213.
38. Sieber JJ, Willig KI, Heintzmann R, Hell SW, Lang T (2006) The SNARE motif is essential for the formation of syntaxin clusters in the plasma membrane. *Biophys J* 90:2843–2851.
39. Baumgart T, Hess ST, Webb WW (2003) Imaging coexisting fluid domains in biomembrane models coupling curvature and line tension. *Nature* 425:821–824.
40. Verhage M, *et al.* (2000) Synaptic assembly of the brain in the absence of neurotransmitter secretion. *Science* 287:864–869.
41. Harrison SD, Broadie K, Vandegoor J, Rubin GM (1994) Mutations in the drosophila rop gene suggest a function in general secretion and synaptic transmission. *Neuron* 13:555–566.
42. Weimer RM, *et al.* (2003) Defects in synaptic vesicle docking in unc-18 mutants. *Nat Neurosci* 6:1023–1030.
43. Melia TJ (2007) Putting the clamps on membrane fusion: How complexin sets the stage for calcium-mediated exocytosis. *FEBS Lett* 581:2131–2139.
44. Braeckmans K, Peeters L, Sanders NN, De Smedt SC, Demeester J (2003) Three-dimensional fluorescence recovery after photobleaching with the confocal scanning laser microscope. *Biophys J* 85:2240–2252.
45. Lopez A, Dupou L, Altibelli A, Trotard J, Tocanne JF (1988) Fluorescence recovery after photobleaching (FRAP) experiments under conditions of uniform disk illumination. Critical comparison of analytical solutions, and a new mathematical method for calculation of diffusion coefficient D. *Biophys J* 53:963–970.